Performance analysis of heat pump based on a new solar air-source heat pump heating system

Liang Caihua　Zhang Xiaosong　Zhu Xia　Li Xiuwei

(School of Energy and Environment, Southeast University, Nanjing 210096, China)

Abstract: To further improve the utilization efficiency of solar energy and the performance of solar heat pump heating systems, a new heating mode of a solar air-source heat pump(SASHP) is proposed, and the characteristics and performance of the heat pump part of this new heating system are studied. Based on a SASHP with 10 kW, the mathematical model of this system is built, and the characteristics and performance are concluded from the simulation analysis at different environmental temperatures and output water temperatures. The results show that the performance of heat pumps can be greatly improved based on the new SASHP. When the environmental temperature is 7 ℃, the coefficient of performance (COP) of the air-source heat pump (ASHP) can be increased by 26% at most. This paper sets up a base for further study on the heating system with this new SASHP in the heating season.

Key words: solar energy; air-source heat pump; heating mode; performance; simulation

Solar energy is a kind of endless and clean energy. However, it may be largely affected by season and weather, which causes that direct application in various solar systems is limited to a certain extent. With a small amount of high-grade electric energy to drive, a heat pump can effectively absorb low-grade heat energy from low temperature heat sources and then pass it onto high temperature heat sources, and, thereby, save high-grade energy. A combination of solar energy and heat pump technology can effectively solve the problems caused by the thinness and intermittence of solar energy.

Since the 1950s, domestic and overseas scholars have made many studies on various solar heat pump systems[1–3]. Hawlader et al. [4] set up an experimental platform for the study of the solar heat pump(SHP) and tested the performance of the system in the circulation under the weather conditions of Singapore. Aye et al. [5] compared the performance of the solar heat water system, the ASHP and the SASHP in different cities of Australia and made economic analyses. Georgiev[6] figured out the influence of various parameters of a solar collector on system performance in the experiments with the solar collector as the heat source of the heat pump. Kaygusuz[7] performed a theoretical study on the SHP, which was equipped with phase-change heat storage device, and obtained the COP value of the system by experi-

ments during the heating season. Zhao et al. [8] performed theoretical analysis and experimental study on a series solar heat pump heat water system, which was supported by a vacuum tube heat collector, and the results showed that this system can run stably throughout the whole year. Yu et al. [9] built up an experimental platform of the SHP and a test system, and performed experimental studies on the heating conditions of the SHP in winter; they also obtained the integral heating performance of the system and the performance of main equipment. Kuang et al. [10 – 12] theoretically studied the series indirect expansion and direct expansion solar heat pump.

The current SHP can be classified into a direct expansion type and an indirect expansion type. According to different connection forms in the solar collection circulation and the heat pump circulation, the indirect expansion solar heat pump can be divided into three types: series, parallel and dual heat sources. In the application of solar energy, the three types of heat pumps treat solar energy as the low-grade heat source of heat pumps. The heat pump consumes electric energy to further improve the grade of energy as the cost of applying solar energy. As for the parallel type, applications of solar energy and heat pump systems are independent of each other, so we are unable to improve the performance of heat pump systems by solar energy. A new solar air-source heat pump heating system(SASHPHS) is proposed, which can improve the working conditions of the heat pump and strengthen the performance of solar energy utilization; then we focus on the changes in characteristics and performance parameters of the ASHP in the new SASHPHS, in order to provide a basis for the performance assessment of this new SASHPHS.

1 New Solar Air-Source Heat Pump Heating System

The flow chart of the new SASHPHS is shown in Fig. 1. The whole heating system consists of two parts: the ASHP and the solar collector system. The output water temperature of the system is 45 ℃ and the return water temperature of the system is 40 ℃. In the cycle of hot water supply, the condenser of the ASHP is in series with the solar collector, with the ASHP at the front and the solar collector at the back. The system works in three modes: 1) Single air-source heat pump mode, which is started while the sun is not available or the radiant intensity is low(The available heat of radiation is smaller than or equal to the heat dissipation of the heat collector when the water temperature is 45 ℃ in the solar collector; the available heat of radiation refers to the heat which can be absorbed by water in the solar collector); 2) Combination mode, which is activated when the available heat of radiation is more than the heat dissipation of the heat collector(The water temperature is 45 ℃ in the solar collector, but the available heat is not enough to increase the water
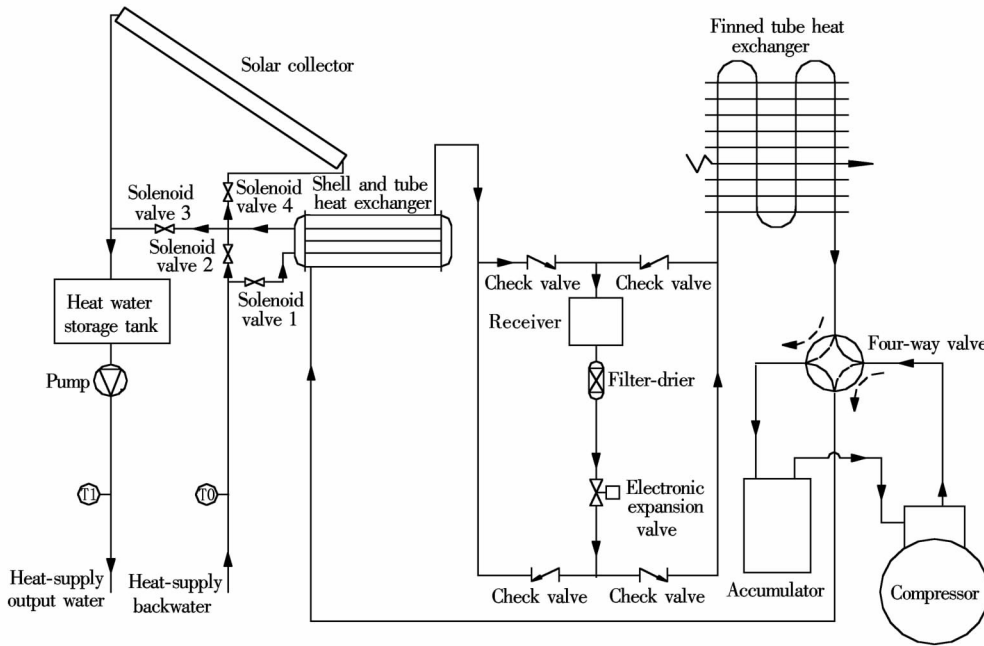
Fig. 1   Flow chart of new solar air-source heat pump heating system

temperature by 5 ℃); 3) Single solar collector mode, which is operated when the solar collector can provide enough heat to increase the water temperature by 5 ℃. The specific process of each mode is as follows:

1) Single air-source heat pump mode: Solenoid valves 2 and 4 are closed; solenoid valves 1 and 3 are opened. Heat-supply backwater passes through solenoid valve 1 and enters the shell and tube heat exchanger, which cools down refrigerant and absorbs the heat, and the temperature increases to 45 ℃. After it comes out from the shell and tube heat exchanger, it passes through solenoid valve 3 to reach the hot water container, and flows out of the system after being pressurized by the pump to supply the air-conditioner terminal.

2) Combination mode: Solenoid valves 2 and 3 are closed; solenoid valves 1 and 4 are opened. Heat-supply backwater passes through solenoid valve 1 and enters the shell and tube heat exchanger; then it cools down the refrigerant, and absorbs the heat and raises the temperature. After it comes out from the shell and tube heat exchanger, it passes through solenoid valve 4 to reach the solar collector to absorb the heat produced by solar energy. When the temperature increases to 45 ℃, it enters the hot water container and flows out the system after being pressurized by the pump to supply the air-conditioner terminal.

3) Solar collector direct heat supply mode: Solenoid valves 1 and 3 are closed; solenoid valves 2 and 4 are opened. Heat-supply backwater passes through solenoid valves 2 and 4, and then directly enters the solar collector to absorb the heat of the sun. When the temperature rises to 45 ℃, it enters the hot water container and flows out the system after being pressurized by the pump to supply the air-conditioner terminal.

The compressor in the ASHP is a variable capacity compressor. In the combination mode, the compressor runs with variable capacity to guarantee that the output water temperature is at 45 ℃. When the radiant intensity is greater, the compressor runs with a smaller capacity, and vice versa. The testing results by a radiant intensity instrument are treated as

the reference for the switching among the three modes.

In the combination mode, with the increase in radiant intensity, the temperature of the output water from the condenser of the ASHP decreases, which means that the condensing pressure and the temperature of the system are decreased, and thus the heat pump performance is improved. To study the operational characteristics and the performance of the heat pump part of this new SASHPHS, we set up a mathematical model of the heat pump based on the new heating system.

2   Establishment of Model of Air-Source Heat Pump System

To study the performance of the heat pump in this heating mode, we establish a mathematical model of the ASHP. The purpose of this paper is to improve the performance parameters of the ASHP at the steady state without paying attention to the dynamic process of the system; we establish the model of the steady stage. The ASHP with 10 kW is selected as the research object under rating working conditions, with an inverter compressor as the compressor of the heat pump, a finned tube heat exchanger as the evaporator in heating, a shell and tube heat exchanger as the condenser, and an electronic expansion valve as the throttle valve. In modeling the ASHP, the following assumptions about the heat exchanger are made: 1) The heat exchange between the shell and tube heat exchanger and the environment is ignored; 2) The pressure inside the heat exchanger and the temperature of the refrigerant inside the two-phase section are constant; 3) Only pure refrigerant is considered; 4) Axial heat transfer is ignored; 5) The refrigerant from each channel of the heat exchanger is fully mixed.

2.1   Model of shell and tube heat exchanger

1) Heat transfer coefficients of refrigerant in single-phase section, α_{sh} and α_s

In the overheated section and the sub-cooled section, the refrigerant-side heat transfer coefficients can be calculated by the standard Dittus-Boelter equation:

$$\alpha_{sh}\ or\ \alpha_{sc} = 0.023\frac{\lambda}{d_i}Re^{0.8}Pr^{0.3} \tag{1}$$

2) Average heat transfer coefficient of refrigerant in two-phase section, $\alpha_{tp\text{-}s}$

Inside the two-phase section, the local heat transfer coefficient $\alpha_{tp\text{-}s}(x)$ can be calculated by the Dobson formula:

$$\alpha_{tp\text{-}s}(x) = 0.023\frac{\lambda_1}{d_i}Re_1^{0.8}\ Pr_1^{0.4}\left(1 + \frac{2.22}{X_{tt}^{0.889}}\right) \tag{2}$$

$$X_{tt} = 0.551\frac{p}{P_{cr}}\left(\frac{1-x}{x}\right)^{0.9} \tag{3}$$

The $\alpha_{tp\text{-}s}$ can be obtained by

$$\alpha_{tp\text{-}s} = \frac{\int_{x_i}^{x_o}\mathrm{d}x}{\int_{x_i}^{x_o}\dfrac{1}{\alpha_{tp\text{-}s}(x)}\mathrm{d}x} \tag{4}$$

3) Heat transfer coefficient of water outside tube, α_o

The shell and tube heat exchanger has a baffle plate and water transfers the heat by vertical and transverse flows outside the tube. The heat transfer coefficient α_o of water outside the tube is

$$\alpha_o = 0.25\frac{\lambda}{d_o}Re^{0.6}Pr^{0.33} \tag{5}$$

2.2　Finned tube heat exchanger model

1) Heat exchange coefficient of refrigerant in overheated section, α_{sh}

Inside the overheated section, refrigerant exists in the form of overheated steam and flows inside the tube are turbulent. The refrigerant heat exchange α_{sh} can be calculated by the Petukhov-Popov formula:

$$\alpha_{sh} = \frac{\lambda_v}{d_i}\frac{\dfrac{f}{8}Re_vPr_v}{1.07 + 12.7\left(\dfrac{f}{8}\right)^{0.5}(Pr_v^{2/3} - 1)} \tag{6}$$

$$f = (1.82\lg Re_v - 1.64)^{-2} \tag{7}$$

2) Average heat exchange coefficient of refrigerant in two-phase section, $\alpha_{tp\text{-}f}$

Inside the two-phase section, the heat exchange coefficient changes with the length of the section. Therefore, the average heat exchange coefficient in the two-phase section $\alpha_{tp\text{-}f}$ can be obtained by computing integrative local heat exchange coefficients in the range of dryness of the evaporator. The formula of the local heat exchange coefficient $\alpha_{tp\text{-}f}(x)$ is as follows:

$$\alpha_{tp\text{-}f}(x) = \frac{3.0}{X_{tt}^{2/3}}\alpha_1 \tag{8}$$

$$X_{tt} = \left(\frac{\mu_1}{\mu_v}\right)^{0.1}\left(\frac{1-x}{x}\right)^{0.9}\left(\frac{\rho_v}{\rho_1}\right)^{0.5} \tag{9}$$

where α_1 stands for the heat exchange coefficient when the refrigerant is at a pure liquid phase. The calculation by the standard Dittus-Boelter formula is as follows:

$$\alpha_1 = 0.023Re_1^{0.8}\ Pr_1^{0.4}\frac{\lambda_1}{d_i} \tag{10}$$

The average heat exchange coefficient of the whole evaporator can be obtained by

$$\alpha_{tp\text{-}f} = \frac{\int_{x_i}^{x_o}\mathrm{d}x}{\int_{x_i}^{x_o}\dfrac{1}{\alpha_{tp\text{-}f}(x)}\mathrm{d}x} \tag{11}$$

3) Air-side heat exchange coefficient α_k

The air-side heat exchange adopts the integrative associative formula of plain and integral finned tube exchange:

$$Nu = 0.982Re^{0.424}\left(\frac{s}{d_b}\right)^{-0.0887}\left(\frac{Ns_2}{d_b}\right)^{-0.1590} \tag{12}$$

2.3　Model of compressor

Suppose that the absorption pressure is the evaporation pressure, and the discharge pressure is the condensation pressure, respectively. The refrigerant circulating load G_{com} is determined by the actual inspiratory volume of the compressor and the refrigerant specific volume at the entry:

$$G_{com} = \frac{\eta_v V_{th}}{v_1} \tag{13}$$

The theoretical capacity of the compressor is

$$V_{th} = \frac{V_{com}n}{60} \tag{14}$$

2.4　Model of electronic expansion valve

Under steady working conditions, the flux of the electronic expansion valve is

$$m_v = C_v A_v\sqrt{\rho_{v,i}(p_{v,i} - p_{v,o})} \tag{15}$$

3　Results and Discussion

In the new SASHPHS, when without sunshine, the heating system performs the direct heating mode of air-source heat pumps; when with sunshine, the system mainly performs the combined heating mode of solar and air-source heat pumps (In this mode, the heat in the heating system is supplied by the solar collector and the ASHP). The heating capacity of the system designed by us is 10 kW under the rating working conditions. As the heating system ignores the function of stored heat, the heating capacity of the ASHP is also 10 kW under the rating working conditions. The rating working conditions of heat pumps include: the dry-bulb temperature is 7 ℃, and the wet-bulb temperature is 6 ℃. The output water temperature and the return temperature of the heating system are relatively maintained at 45 and 40 ℃. The frequency of the compressor in the ASHP varies from 15 to 110

Hz. In the combined heating mode of solar and air-source heat pumps, as the inverter compressor is limited by the lowest operation frequency (15 Hz), the lowest output water temperature is 41 ℃ in the simulation of the performance of the ASHP.

The influence of the solar collector on the ASHP is mainly represented as follows: In the combined heating mode of solar and air-source heat pumps, the ASHP can run at small capacity, while the temperature in the condenser is decreased, so working conditions are improved. The variety of solar radiation intensity results in the changes of the output water temperature from the ASHP; namely, given that the area of the solar collector is constant, different output water temperatures in the ASHP are related to different solar radiation intensities. Based on the simulation of the mathematical model of the ASHP, the curves of the output water temperature and performance parameters of the ASHP are shown in Figs. 2 to 5.
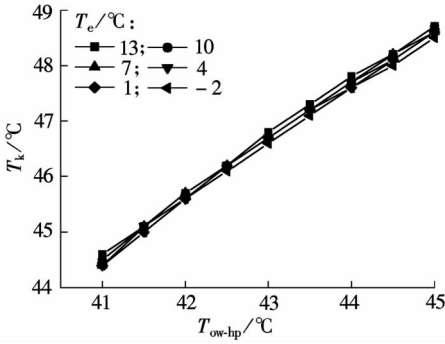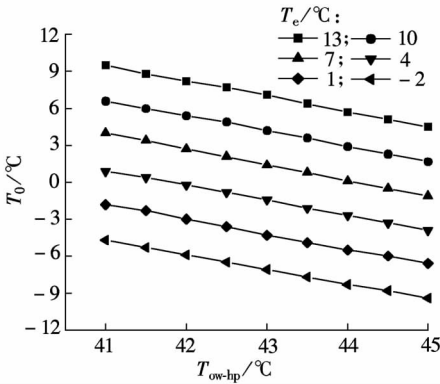

Fig. 2   Variety of T_k at different $T_{ow\text{-}hp}$ and T_e

Fig. 3   Variety of T_0 at different $T_{ow\text{-}hp}$ and T_e
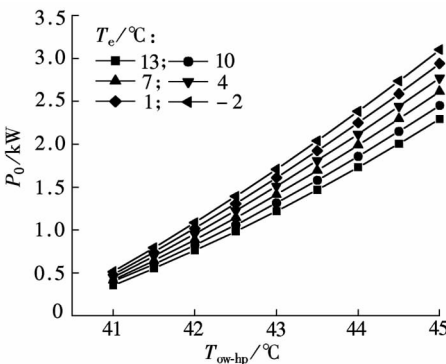
Fig. 4   Variety of P_0 at different $T_{ow\text{-}hp}$ and T_e
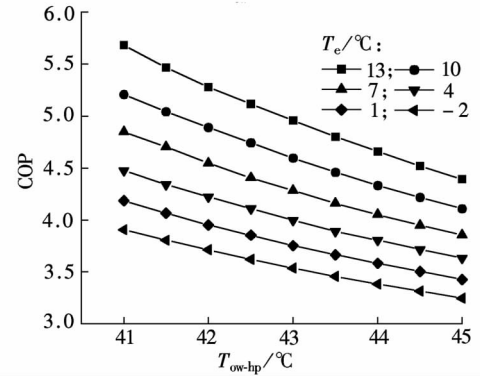

Fig. 5   Variety of COP of heat pump at different $T_{ow\text{-}hp}$ and T_e

Figs. 2 and 3 show the curves of the condensation temperature T_k and the evaporation temperature T_0 at different output water temperatures of the heat pump $T_{ow\text{-}hp}$ and environmental temperatures T_e. From Fig. 2, we can see that T_k decreases with the decrease in $T_{ow\text{-}hp}$, which proves that the condensation conditions of the ASHP are improved. As the water flow of the condenser in the ASHP is constant, while $T_{ow\text{-}hp}$ decreases, the heating power of the ASHP also decreases, and the flow of the refrigerant, the heat exchange temperature difference and T_k decrease. From Fig. 2, it is concluded that T_e has little influence on T_k. From Fig. 3, we can see that at a specific temperature, while $T_{ow\text{-}hp}$ decreases, T_0 rises. The main reason is that while $T_{ow\text{-}hp}$ decreases, the flow of refrigerant decreases. As for the same finned tube evaporator, the heat exchange area of refrigerant per unit mass increases in the evaporator, and the heat exchange temperature difference decreases; thereby, T_0 rises and the systemic performance is improved. From Fig. 3, it is concluded that at different T_e and $T_{ow\text{-}hp}$, T_0 has the same trend.

Fig. 4 indicates the curves of power consumption of the compressor in the ASHP(P_0) at different $T_{ow\text{-}hp}$ and T_e. As shown in Fig. 4, with the decrease in $T_{ow\text{-}hp}$, P_0 tends to decrease. When T_e is 7 ℃, $T_{ow\text{-}hp}$ decreases from 45 to 41 ℃ and P_0 decreases from 2. 61 to 0. 42 kW. Meanwhile, with the decrease of T_e, P_0 changes rapidly with $T_{ow\text{-}hp}$.

Fig. 5 indicates the COP curves of the ASHP at different $T_{ow\text{-}hp}$ and T_e. It shows that for a specific T_e, the COP value has a remarkable increase with the decrease in $T_{ow\text{-}hp}$. With the increase in T_e, the COP tends to increase faster and faster. With T_e at 7 ℃, when $T_{ow\text{-}hp}$ decreases from 45 to 41 ℃, the COP of the ASHP increases from 3. 86 to 4. 85, indicating that the performance of the ASHP is remarkably improved. By the analysis, we conclude that it is mainly because, with the decrease in $T_{ow\text{-}hp}$, T_k also decreases while T_0 increases and, thereby, the working conditions of heat pumps are improved.

Fig. 6 shows the curves of the COP improvement rate of the ASHP(ΔCOP) at different $T_{ow\text{-}hp}$ and T_e. From Fig. 6, we can see that with the decrease in $T_{ow\text{-}hp}$, the COP improvement rate of the machine set increases. With T_e of 7 ℃, when $T_{ow\text{-}hp} = 41$ ℃, the COP value is 26% higher than that when $T_{ow\text{-}hp} = 45$ ℃. Meanwhile, Fig. 6 indicates that with the increase in T_e, the ΔCOP increases faster with the decrease in $T_{ow\text{-}hp}$. Thus, it can be seen that when T_e is higher, the improvement of performance of the ASHP is more remarkable.
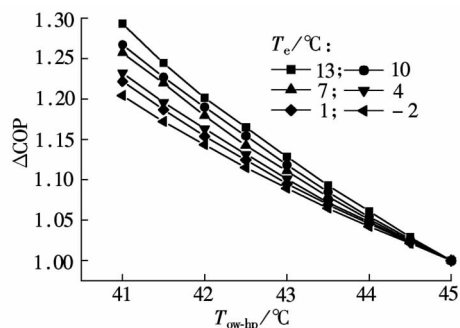
Fig. 6 Variety of ΔCOP at different $T_{\text{ow-hp}}$ and T_e

4　Conclusion

This paper proposes a new solar air-source heat pump heating system and analyzes the principles and the processes of this new heating system. The performance improvement is studied for the air-source heat pump in the heating system. Its mathematical model is built based on the air-source heat pump with 10 kW. With the model, the performance of the air-source heat pump at different environmental temperatures and output water temperatures is simulated. The influences of environmental temperature and output water temperature of heat pumps on evaporating temperature, condensation temperature, the power consumption of the compressor and the COP value of the system are obtained. This study provides a base for further study on the heating performance of this new system in the heating season. The results show that in the heating mode of the new solar air-source heat pump, the air-source heat pump performance is greatly improved. At an environmental temperature of 7 ℃, when the output water temperature is 41 ℃, the COP value is 26% higher than that when the output water temperature is 45 ℃. With the increase in environmental temperature, the COP improvement rate of the heat pump system also increases. Thus, it can be concluded that the heating mode of this new solar air-source heat pump has better energy-saving performance.

References

[1] Chaturvedi S K, Chen D T, Kheireddine A. Thermal performance of a variable capacity direct expansion solar-assisted heat pump[J]. *Energy Conversion & Management*, 1998, **39**(3/4):181 － 191.

[2] Day A R, Karayiannis T G. Solar-assisted heat pump research and development [J]. *Building Service Engineering Research & Technology*, 1994, **15**(2):71 － 80.

[3] Freeman T L, Mitchell J W, Audit T E. Performance of combined solar-heat pump systems [J]. *Solar Energy*, 1979, **22**(2):125 － 135.

[4] Hawlader M, Chou S K, Ullah M. The performance of a solar assisted heat pump water heating system[J]. *Applied Thermal Engineering*, 2001, **21**(10):1049 － 1065.

[5] Aye L, Charters W, Chachana C. Solar heat pump systems for domestic hot water[J]. *Solar Energy*, 2002, **73**(3):169 － 175.

[6] Georgiev A. Testing solar collectors as an energy source for a heat pump[J]. *Renewable Energy*, 2008, **33**(4):832 － 838.

[7] Kaygusuz K. Experimental and theoretical investigation of a solar heating system with heat pump[J]. *Renewable Energy*, 2000, **21**(1):79 － 102.

[8] Zhao J, Ma Y T, Zheng Z H, et al. The experimental study on solar assisted heat pump system for hot water supply[J]. *Acta Energiae Solaris Sinica*, 1993, **14**(4):306 － 310. (in Chinese)

[9] Yu L Q, Kuang Y H, Shi Z G, et al. Measurement result of the solar assisted heat of pump system[J]. *Construction Machinery for Hydraulic Engineering & Power Station*, 2004, **4**(3):1 － 4. (in Chinese)

[10] Kuang Y H, Wang R Z, Yu L Q. Experimental study of solar assisted heat pump system for heat supply[J]. *Acta Energiae Solaris Sinica*, 2002, **23**(4):408 － 413. (in Chinese)

[11] Kuang Y H, Sumathy K, Wang R Z. Study on a direct-expansion solar-assisted heat pump water heating system[J]. *International Journal of Energy Research*, 2003, **27**(5):531 － 548.

[12] Kuang Y H, Wang R Z. Performance of a multi-functional direct-expansion solar assisted heat pump system[J]. *Solar Energy*, 2006, **80**(7):795 － 803.

基于新型太阳能空气源热泵供热系统的热泵性能研究

梁彩华　　张小松　　朱　霞　　李秀伟

（东南大学能源与环境学院,南京 210096）

摘要:为进一步提高太阳能利用效率和太阳能辅助空气源热泵供热系统的性能,提出了一种新型太阳能空气源热泵供热系统,并研究了该供热系统的性能和特性.基于自行设计的 10 kW 空气源热泵,建立了供热系统的数学模型,通过模拟得出了不同环境温度和出水温度下供热系统的运行特性和性能规律.结果表明:基于新型太阳能辅助空气源热泵供热系统,热泵的性能得到较大的提高.当环境温度为 7 ℃时,空气源热泵的 COP 最大可增加 26%.这为进一步研究新型太阳能辅助空气源热泵供热系统在供暖季节的性能奠定了基础.

关键词:太阳能;空气源热泵;供热模式;性能;模拟

中图分类号:TB657